Electronic Supplementary Material (ESI) for Journal of Materials Chemistry C.

Supplementary Information

Observation of planar Hall effect in topological insulator candidate $Ni_3Bi_2Se_2$

Yuzhe Ma,[ab] Wen Sun,[ab] Qiunan Xu[c], Xinming Wang,[bd] Aisha Aqeel[efg] and Guowei Li [ab]

a. CAS Key Laboratory of Magnetic Materials and Devices, Ningbo Institute of Materials Technology and Engineering, Chinese Academy of Sciences, Ningbo 315201, China. Email: liguowei@nimte.ac.cn

b. University of Chinese Academy of Sciences, 19 A Yuquan Rd, Shijingshan District, Beijing 100049, China

c. Qingdao Institute for Theoretical and Computational Sciences Shandong University Qingdao 266237, China

d. Public Technical Service Center, Ningbo Institute of Materials Technology and Engineering, Chinese Academy of Sciences, Ningbo 315201, China

e. Physics Department, Technical University of Munich, Garching, Germany

f. Munich Center for Quantum Science and Technology (MCQST), Munich, Germany

g. Institute of Physics, University of Augsburg, Augsburg, Germany

Table S1. The parities for each time reversal invariant momentum in $Ni_3Bi_2Se_2$.

δ (0 0 0)	δ (0.5 0 0)	δ (0 0.5 0)	δ (0.5 0.5 0)
-	+	+	-
δ (0 0 0.5)	δ (0.5 0 0.5)	δ (0 0.5 0.5)	δ (0.5 0.5 0.5)
+	+	+	-

By using the method in **[1]**, we get the Z2 invariant of $Ni_3Bi_2Se_2$ is (1;111), which indicates $Ni_3Bi_2Se_2$ is a strong topological insulator. The parities for each time reversal invariant momentum are listed in Table S1.

Table S2. Crystallographic data and structure refinement parameters for $Ni_3Bi_2Se_2$.

Formula	$Ni_3Bi_2Se_2$
Formula weight	752.01
T (K)	223
Space group	*C*2/*m*
Unit cell dimensions	*a* = 11.1858(5) Å
	b = 8.1601(5) Å
	c = 8.0756(5) Å
Volume	537.07(6) $Å^3$
Z	4
Density (calculated)	9.3 g/cm^3
Goodness-of-fit on F^2	1.081
Final R indices [I > 2sigma(I)]	R1 = 0.0319,
	wR2 = 0.0928
R indices (all data)	R1 = 0.0327,
	wR2 = 0.0934

Table S3. Atomic coordinates and equivalent isotropic displacement parameters for $Ni_3Bi_2Se_2$. U_{eq} is defined as one third of the trace of the orthogonalized U_{ij} tensor.

atom	x	y	z	U_{eq} ($Å^2$)
Bi1	0.24931(7)	0.50000	0.24327(10)	0.0179(2)
Bi2	0.28285(7)	0.50000	0.79880(11)	0.0192(2)
Se1	0.47286(2)	0.21827(5)	0.69044(9)	0.0183(3)
Ni3	0.50000	0.22650(2)	1.00000	0.0202(4)
Ni1	0.48120(2)	0.50000	0.70950(4)	0.0224(5)
Ni2	0.75000	0.25000	1.00000	0.0202(5)

Table S4. Selected interatomic distances [Å] in $Ni_3Bi_2Se_2$.

Bi1-Ni3	2.7475 (13) ×2	Bi2-Ni1	2.8940(2)
Bi1-Ni1	2.7430(2)	Bi2-Ni2	2.7847(4) ×2
Bi1-Ni1	2.7361(17)	Se1-Ni3	2.3036(11)
Bi1-Ni2	2.8359(4) ×2	Se1-Ni1	2.3017(12)
Bi2-Bi2	3.5404(12)	Se1-Ni2	2.3045(11)
Bi2-Ni3	2.8483(15) ×2	Ni3-Ni2	2.8029(17) ×2
Bi2-Ni1	2.7671(17)		

Table S5. Anisotropic displacement parameters [Å^2] for $Ni_3Bi_2Se_2$. The anisotropic displacement factor exponent takes the form: $-2\pi^2 [h^2 a^{*2} U^{11} + ... + 2 h k a^* b^* U^{12}]$.

	U^{11}	U^{22}	U^{33}	U^{23}	U^{13}	U^{12}
Bi1	0.0178(3)	0.0180(1)	0.0182(4)	0	0.0124(3)	0
Bi2	0.0191(4)	0.0191(3)	0.0195(4)	0	0.0133(3)	0
Se1	0.0182(6)	0.0183(5)	0.0172(6)	0.0002(4)	0.0116(5)	-0.0008(4)
Ni3	0.0197(10)	0.0204(10)	0.0258(13)	0	0.0138(9)	0
Ni1	0.0222(11)	0.0204(10)	0.0258(13)	0	0.0168(1)	0
Ni2	0.0180(10)	0.0227(10)	0.0190(11)	-0.0016(7)	0.0123(9)	-0.0021(7)

Table S6. The energy-dispersive X-ray spectroscopy (EDX) analyses for $Ni_3Bi_2Se_2$ single crystals.

Sample	Point	Ni atomic ratio (%)	Bi atomic ratio (%)	Se atomic ratio (%)
1	①	42.76	28.72	28.52
	②	42.32	28.36	28.32
	③	41.98	28.94	29.08
	④	43.01	29.02	27.79
	⑤	42.29	27.95	27.76
2	①	43.24	29.01	27.75
	②	42.84	28.48	28.68
	③	43.11	28.59	28.30
	④	42.53	27.89	29.58
	⑤	43.01	29.09	27.81

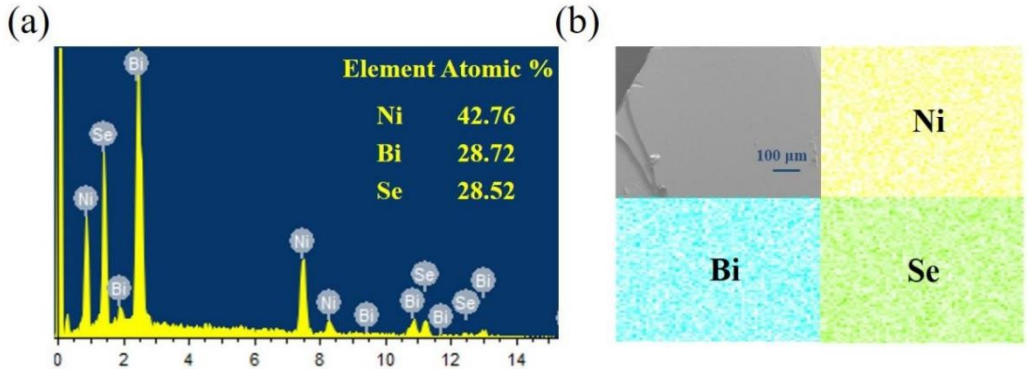

Fig. S1 (a) The EDX spectrum of $Ni_3Bi_2Se_2$ crystal displaying with a stoichometric ratio. (b) The SEM and Ni, Bi, Se elemental mapping images of $Ni_3Bi_2Se_2$ single crystal.

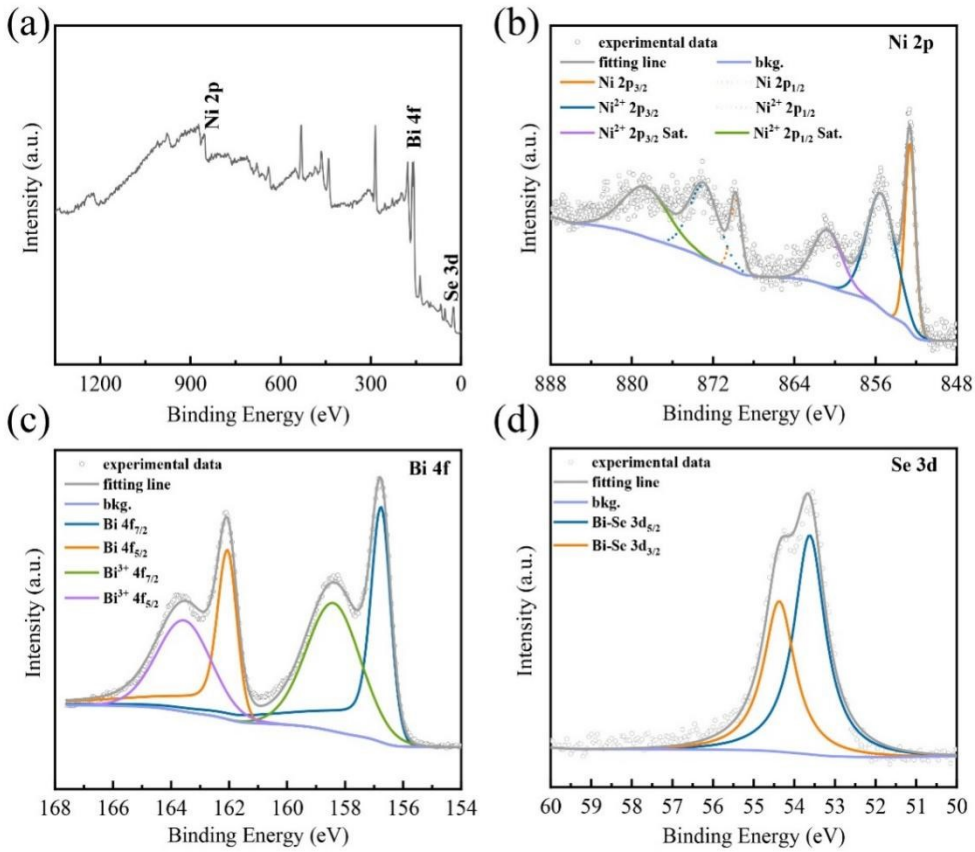

Fig. S2 (a) The XPS survey spectrum of the bulk single crystal. Detailed XPS spectra of (b) Ni 2p, (c) Bi 4f, and (d) Se 3d.

Fig. S2(a) shows the X-ray photoelectron spectroscopy (XPS) survey of $Ni_3Bi_2Se_2$, demonstrating the presence of Ni, Bi, and Se in the single crystal, which is consistent with the results of EDX. As shown in Fig. S2(b), two peaks at binding energies of 855.43 and 872.88 eV can be assigned to Ni $2p_{3/2}$ and Ni $2p_{1/2}$, respectively. The broad peaks at 860.72 and 878.65 eV correspond to the Ni $2p_{3/2}$ and Ni $2p_{1/2}$ satellites. For the Bi 4f spectrum, the Bi $4f_{7/2}$ and Bi $4f_{5/2}$ peaks with binding energies of 158.4 and 163.55 eV correspond to the Bi^{3+} configuration in $Ni_3Bi_2Se_2$ (Fig. S2(c)). Additionally, the two peaks at 53.62 eV and 54.37 eV observed in Figure S2(d) suggest a possible 2- valence state of Se in $Ni_3Bi_2Se_2$. All these results indicate the successful preparation of $Ni_3Bi_2Se_2$.

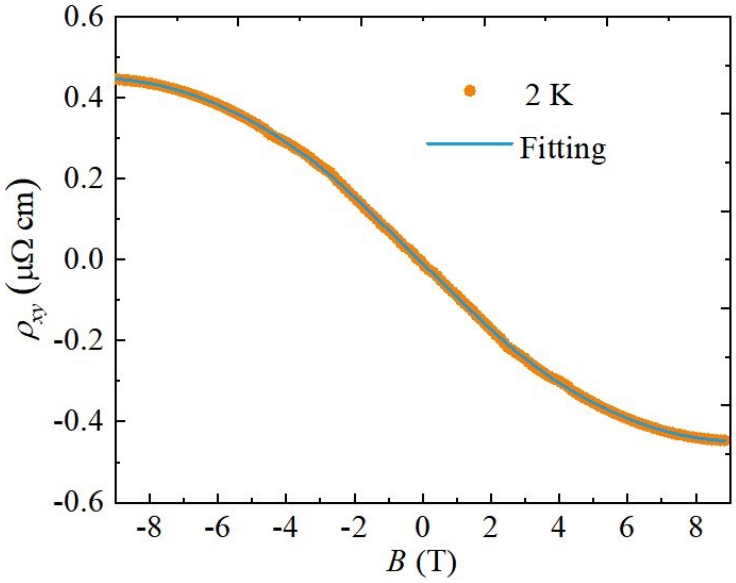

Fig. S3 The magnetic-field-dependent ρ_{xy} at 2 K, and the blue solid line represents the fitting result by two-band model.

According to the two-band model, the Hall resistivity under a magnetic field can be fitted by the equation (1).

$$\rho_{xy} = \frac{1}{e}\frac{\mu_h^2\mu_e^2\,(n_h - n_e)B^3 + \left(\mu_h^2 n_h - \mu_e^2 n_e\right)B}{\mu_h^2\mu_e^2\,(n_h - n_e)^2B^2 + (\mu_h n_h + \mu_e n_e)^2} \qquad (1)$$

Where n_e and n_h are the concentration of electron and hole, u_e and u_h the mobility of electron and hole. Subsequently, the equation can be written as follows.

$$\rho_{xy} = \frac{aB^3 + bB}{cB^2 + 1} \qquad (2)$$

where a, b, and c can be expressed as follows.

$$a = \frac{e\mu_h^2\mu_e^2(n_h - n_e)}{\sigma_0^2} \qquad b = \frac{e(\mu_h^2 n_h - \mu_e^2 n_e)}{\sigma_0^2} \qquad (3)$$

$$c = \frac{e^2\mu_h^2\mu_e^2(n_h - n_e)^2}{\sigma_0^2} \qquad \sigma_0 = e(\mu_h n_h + \mu_e n_e)$$

σ_0 is the conductivity at zero field ($\sigma_0 = 1/\rho_0$), which can be measured independently. Then, by fitting $\rho_{xy}(B)$ using equations (1) and (2), n_e (n_h) and μ_e (μ_h) at different temperatures were obtained.

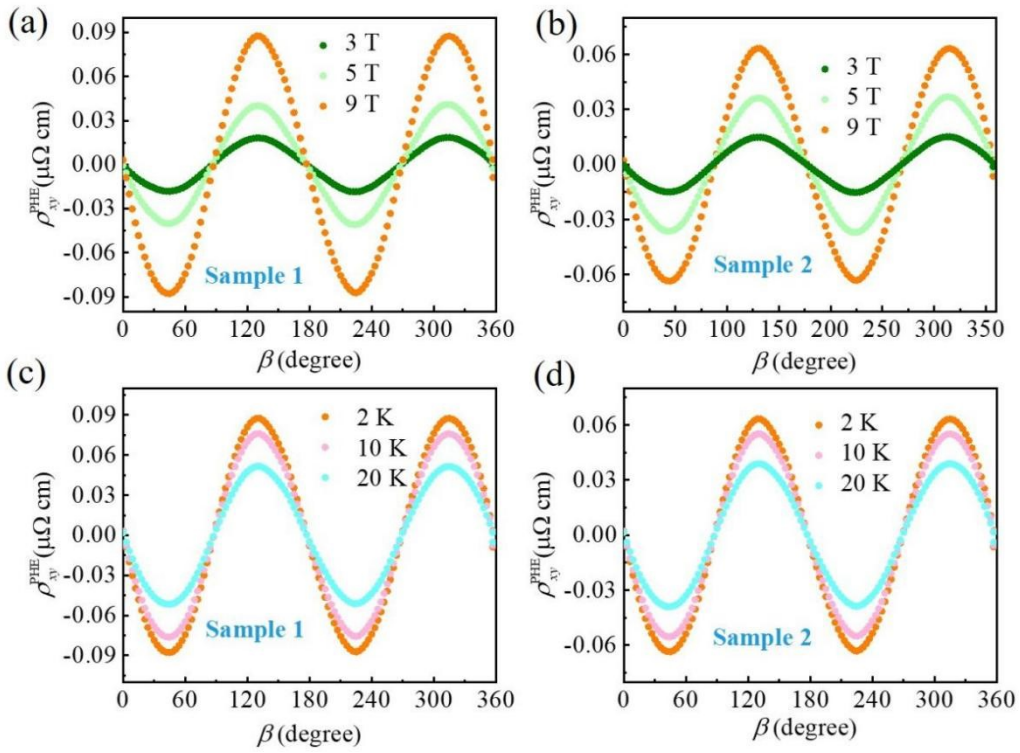

Fig. S4 (a) (b) The planar Hall resistivity under different magnetic fields (3 T, 5 T, 7 T) at 2 K for sample 1 and sample 2. (c) (d) The angle-dependent planar Hall resistivity under different temperatures (2 K, 10 K, 20 K) at 9 T.

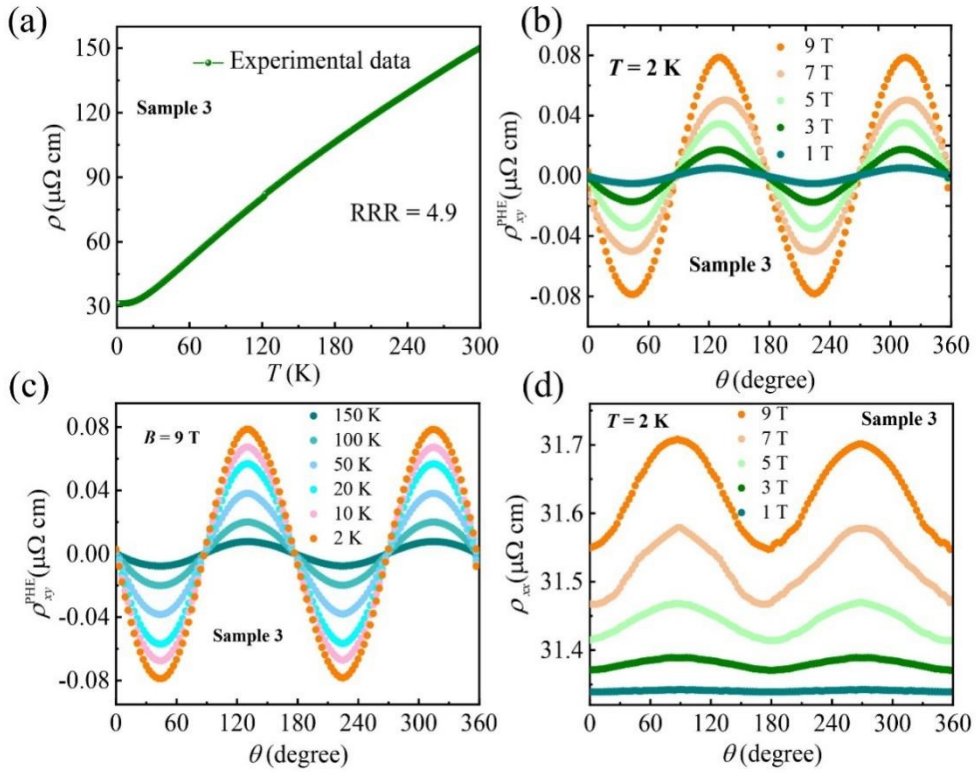

Fig. S5 (a) The temperature-dependent resistivity for $Ni_3Bi_2Se_2$ single crystal measured with I // ab plane. (b) The angle-dependent planar Hall resistivity under different magnetic fields at 2 K. (c) The PHE data under various temperatures at 9 T. (d) The angle dependence of planar resistivity at different magnetic fields for T = 2 K.

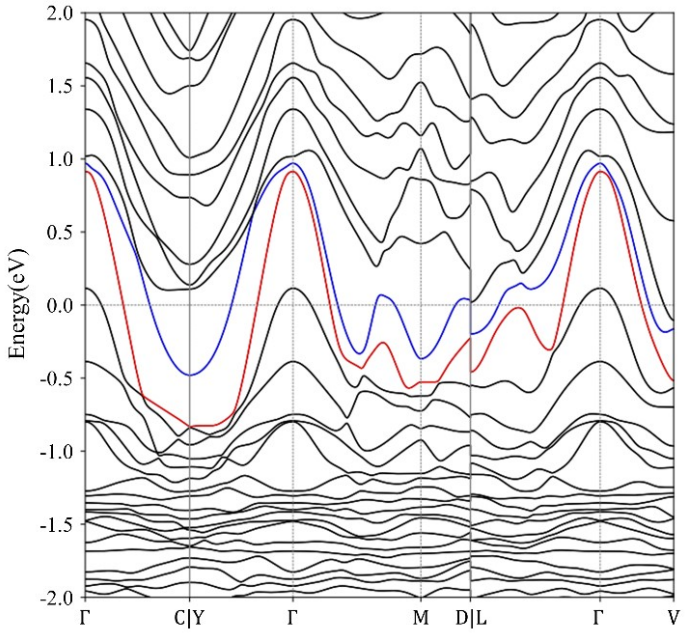

Fig. S6 The calculated electronic band structure of $Ni_3Bi_2Se_2$ with spin-orbit coupling.

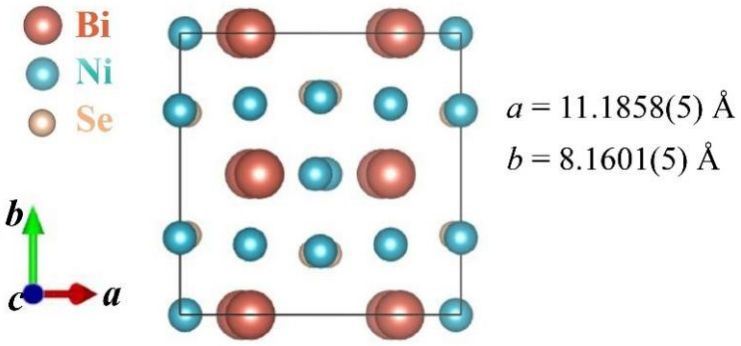

Fig. S7 The schematic single crystal structure of $Ni_3Bi_2Se_2$ along *c* axis.

Reference

[1] Liang Fu and C. L. Kane. *Phys. Rev. B*, 2007, **76**, 045302.